Post-conference fieldtrip, October 21-24, 2019: Ediacaran and Terreneuvian strata surrounding the Villuercas-Ibores-Jara UNESCO Global Geopark

Guía de campo post-congreso, 21-24 de Octubre de 2019: Ediacárico y Terreneuviense en los alrededores del Geoparque de la UNESCO Villuercas-Ibores-Jara

J.J. Álvaro[1], S. Jensen[2], T. Palacios[2]

[1]Instituto de Geociencias (CSIC-UCM), Dr. Severo Ochoa 7, 28040 Madrid, Spain. Email: jj.alvaro@csic.es, ORCID ID: http://orcid.org/0000-0001-6294-1998
[2]Área de Paleontología, Facultad de Ciencias, Universidad de Extremadura, 06071 Badajoz, Spain. Email: soren@unex.es, medrano@unex.es; ORCID ID: http://orcid.org/0000-0003-4573-9282, http://orcid.org/0000-0002-4917-0559

ABSTRACT

One of the corners of the geographical maps that link the provinces of Badajoz, Cáceres and Toledo contains some key outcrops necessary to understand the Ediacaran-Cambrian transition in the Central-Iberian Zone. In the cores of the Extremenian Anticlinorium and the Ibor and Valdelacasa anticlines, the Lower Alcudian-Domo Extremeño Supergroup (including the diamictites of the Orellana Formation), the most spectacular microbial reefs with *Cloudina* of the Villarta Formation, and the palaeoichnological base of the Cambrian in the Arrocampo Formation (both the Villarta and Arrocampo formations belong to the Ibor Group) stand out. The exposures that were traditionally considered as representatives of the Precambrian-Cambrian boundary and base of the Cordubian regional Stage are located in the lower member of the Pusa Formation, unconformably overlying the Ibor Group, and are considered at present as intra-Terreneuvian in age.

Keywords: Ediacaran, Cambrian, Palaeoichnological record, *Cloudina*-bearing reefs, Cadomian.

RESUMEN

Una de las esquinas de los mapas geográficos que enlazan las provincias de Badajoz, Cáceres y Toledo contiene unos afloramientos claves para entender el tránsito Ediacárico-Cámbrico de la Zona Centroibérica. En los núcleos del Anticlinorio Extremeño y de los Anticlinales de Ibor y Valdelacasa afloran el Supergrupo del Alcudiense inferior-Domo Extremeño (donde destacan las diamictitas de la Formación de Orellana), los arrecifes microbianos más espectaculares con *Cloudina* de la Formación de Villarta y la base paleoicnológica del Cámbrico en la Formación de Arrocampo (las dos últimas formaciones pertenecen al Grupo de Ibor). Los afloramientos que tradicionalmente se consideraban como representantes del límite Precámbrico-Cámbrico y base del piso regional Cordubiense se sitúan en el miembro inferior de la Formación del Pusa, suprayacentes al Grupo de Ibor y considerados actualmente como intra-terreneuvienses.

Palabras clave: Ediacárico, Cámbrico, Registro paleoicnológico, Arrecifes con *Cloudina*, Cadomiense.

Introduction

The surroundings of the Villuercas-Ibores-Jara UNESCO Global Geopark (Cáceres province, Spain) comprise some key outcrops to constrain the Ediacaran-Cambrian boundary interval in the Iberian Peninsula. The stops of the International Meeting on the Ediacaran-Cambrian Boundary (IMECT), post-conference fieldtrip (October 21-24, 2019) located in the Badajoz, Cáceres and Toledo provinces, are described and illustrated below.

October 21: Lower Alcudian-Domo Extremeño Supergroup

The stops of this day provide examples of sedimentary rocks, including glaciogenic diamictites, from the Lower Alcudian-Domo Extremeño Supergroup, cropping out in the Extremenian Anticlinorium; for stratigraphic setting, see Figure 1.

STOP 1. Zújar dam

The area to be visited is reached by driving south from Guadalupe into the northern regions of the Badajoz Province, south of Orellana la Vieja village. During this drive a vast flat area is crossed by road EX-116. Thousands of cranes pass the winters in this area.

Location and description. Road cut close to lock of Zújar dam, at (WGS 84) 38°54'51"N, 05°24'37"W. This outcrop gives a view of greywacke and shaly sediments typical of the Lower Acudian-Domo Extremeño Supergroup commonly exhibiting vertically oriented fold axes.

STOP 2. Weesenstein-Orellana post-Gaskiers glaciation

(Ulf Linnemann & Agustín Pieren)

In the Cadomian orogen of the NE Bohemian Massif and of SW Iberia a ca. 565 Ma old post-Gaskiers glacial event has been detected (Linnemann *et al*., 2018). Such Ediacaran-aged glaciomarine deposits occur in the Weesenstein and Clanzschwitz groups of the Saxo-Thuringian Zone (Bohemia) and in the Lower Alcudian-Domo Extremeño Supergroup of the southern Central Iberian Zone (Iberian Massif). Both areas are parts of Cadomia situated in the Western and Central European Variscides. A suspect tillite exists in the Armorican Massif at Granville (Normandy; Fig. 2) (Wegmann *et al*., 1950, Wegmann, 1951, Graindor, 1964). Its origin is under discussion and the interpretation as glaciomarine deposit was rejected by Eyles (1990). Glaciomarine sedimentary rocks are characterized by such features as dropstones, flat iron shaped pebbles (*"Bügeleisen-Geschiebe"*), facetted pebbles, dreikanters and zircon grains affected by ice abrasion. For the maximum age of deposition and for provenance determination LA-ICP-MS U-Pb zircon ages were performed. The maximum age of the glaciomarine deposits within a Cadomian back-arc basin based on U-Pb analytics resulted in the youngest detrital zircon populations showing ages of ca. 565 Ma. Described glaciomarine diamictites of Cadomia (Weesenstein, Clanzschwitz and Orellana diamictites) are definitely younger than the ca. 579-581 Ma old Gaskiers glaciation in Newfoundland (Gaskiers) (Pu *et al*., 2016). Linnemann *et al*. (2018) proposed the term Weesenstein-Orellana Glaciation for the new Ediacaran glacial event, named after its most relevant regions of exposure. Palaeogeographically, these glaciomarine diamictites and related sedimentary deposits lie on the periphery of the West African craton (western peri-Gondwana), evidence provided by detrital zircon U-Pb ages and their Hf isotope composition (Linnemann *et al*., 2018). Correlation with similar glaciomarine deposits in the Anti-Atlas (Bou Azzer inlier; Vernhet *et al*., 2012) and Arabia (Vickers-Rich *et al*., 2012) suggests a continued distribution of post-Gaskiers glacial deposits along the Gondwana margin of Northern Africa. The Weesenstein-Orellana Glaciation correlates with the Shuram-Wonoka $\delta^{13}C$ anomaly.

The deposits of the Weesenstein-Orellana glaciation in the Central Iberian Zone. Here we focus, due to the working area of the field workshop, on the Spanish part of the glacial deposits of the Weesenstein-Orellana Glaciation in the Orellana area (Figs. 3-4). The latter one is part of the Central Iberian Zone (Julivert *et al*., 1972). Ovtracht & Tamain (1970) studied the Proterozoic rocks of the Schist and Greywacke Complex in the core of the Alcudia Anticline. They subdivided the Ediacaran sedimentary rocks into "Lower and Upper Alcudian groups" (Fig. 4), subsequently integrated into the so-called "Alcudian Supergroup" (San José *et al*., 1990). These rocks have also been called the Extremenian or Extremeño Dome Group (Álvarez Nava *et al*., 1988), though, despite the name, the unit was defined in another structure further north. Therefore, the term Lower Alcudian-Domo Extremeño Supergroup is selected here (see Álvaro *et al*., 2019). In the surroundings of Orellana, Ediacaran and
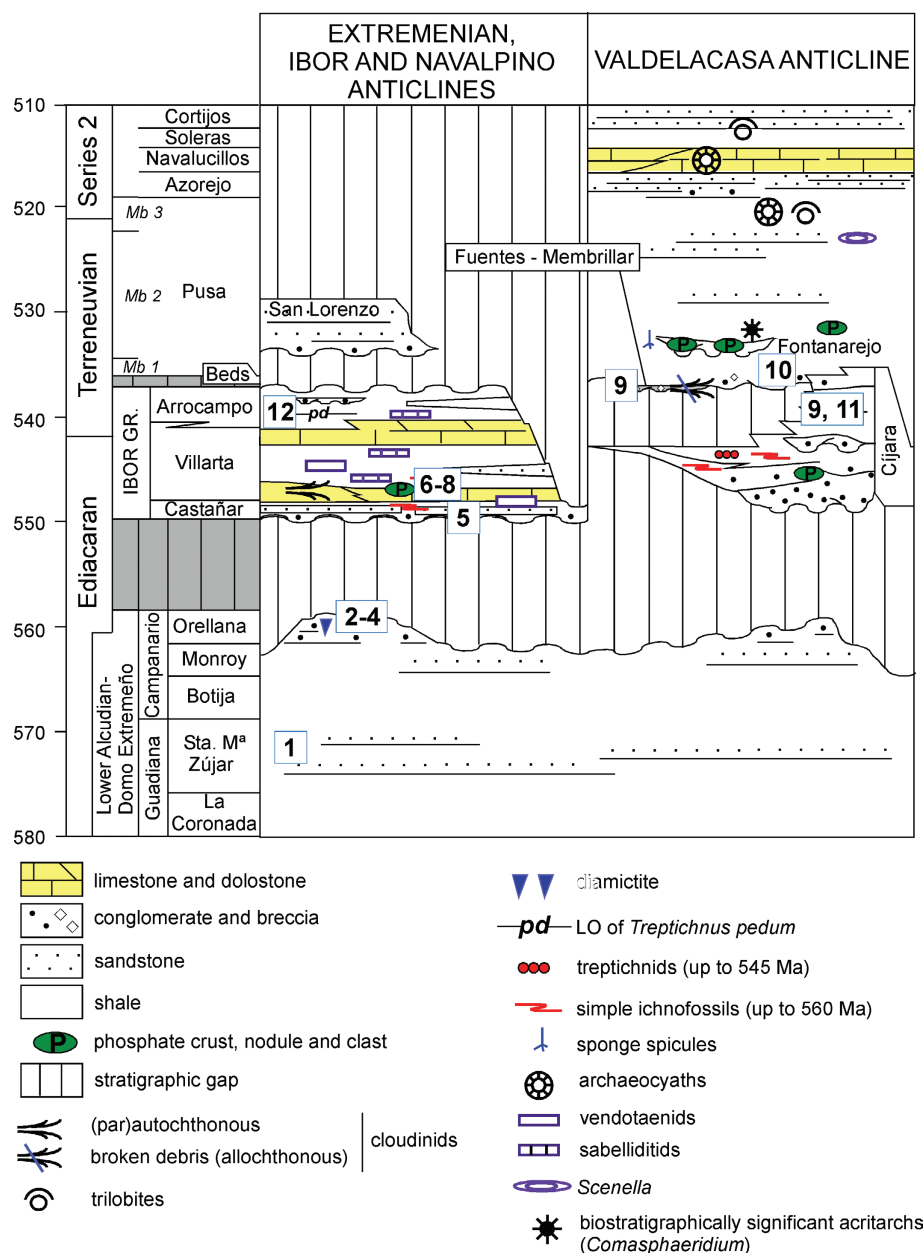
Figure 1.— Stratigraphic sketch of the Extremenian Anticlinorium and the Ibor, Nalvalpino and Valdelacasa anticlines (modified from Álvaro *et al*., 2019) with setting of stops (boxed numbers).

Lower Palaeozoic strata were mapped and studied in detail by Pieren (2000). The exposed Lower Alcudian-Domo Extremeño Supergroup is about 4000 m thick but its base is not exposed. The supergroup is characterized by a monotonous succession of turbidites composed of greywackes and mudstones (Fig. 4). According to García-Hidalgo *et al*. (1993) and Pieren (2000), the supergroup is composed, from bottom to top, of (i) shale and greywacke ("La Coronada Shales formation"), (ii) greywacke, microconglomerate and shale ("Saint Mary of Zújar chapel greywackes and conglomerates formation"), and (iii) shale, diamictite (pebbly mudstone) and greywacke ("Orellana matrix supported conglomerates formation") (Fig. 4). Some greywacke turbidite beds of the second formation are up to 6 m thick and have been used as marker beds during the geological mapping of the region.
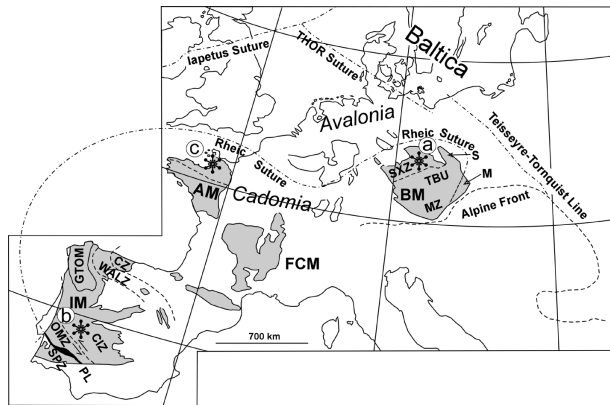
Figure 2.– Location of Variscan massifs in Central and Western Europe: AM- Armorican massif, BM- Bohemian massif, FCM- French Central massif, IM- Iberian massif, M- Moravo-Silesian unit, S- Sudetes. Variscan zones: CIZ- Central Iberian; CZ- Cantabrian, GTOM- Galicia-Tras os Montes, MZ- Moldanubian, OMZ- Ossa Morena, PL- Pulo do Lobo, SPZ- South Portuguese, SXZ- Saxo-Thuringian, TBU- Teplá-Barrandian unit and WALZ- West Atsurian-Leonese Zones. Ediacaran glaciomarine deposits in the Cadomian orogen: a- Weesenstein and Clanzschwitz, b- Orellana, c- suspected tillite of Granville (Wegmann *et al*., 1950; Wegmann, 1951; Graindor, 1964).

The Lower Alcudian-Domo Extremeño Supergroup was folded and locally cleaved during the Cadomian orogenic activity. Generally, a vertical and subvertical L_1 lineation is present, which was generated by a (in the area) non-schistose gentle folding in the late Ediacaran ("intra-Alcudian" or Cadomian deformation). In addition, a Variscan schistose F_1 exists. Most cobbles were oriented parallel to a 70º N dipping L^1 lineation. Some of them were not oriented or almost normal to the L^1 lineation (Pieren, 2000).

STOPS 3 (Orellana reservoir at "Poblado Turístico") and 4 (road Orellana la Vieja to Zújar river reservoir)

(Ulf Linnemann & Agustín Pieren)

Stops 3 (38°59'49.02"N, 5°31'49.97"W) and 4 (38°58'36.10"N, 5°31'19.14"W) are focused on diamictites from the uppermost part the Lower Alcudian-Domo Extremeño Supergroup (Figs. 4, 5A, 5F). These show distinct features indicative of a glaciomarine origin, including
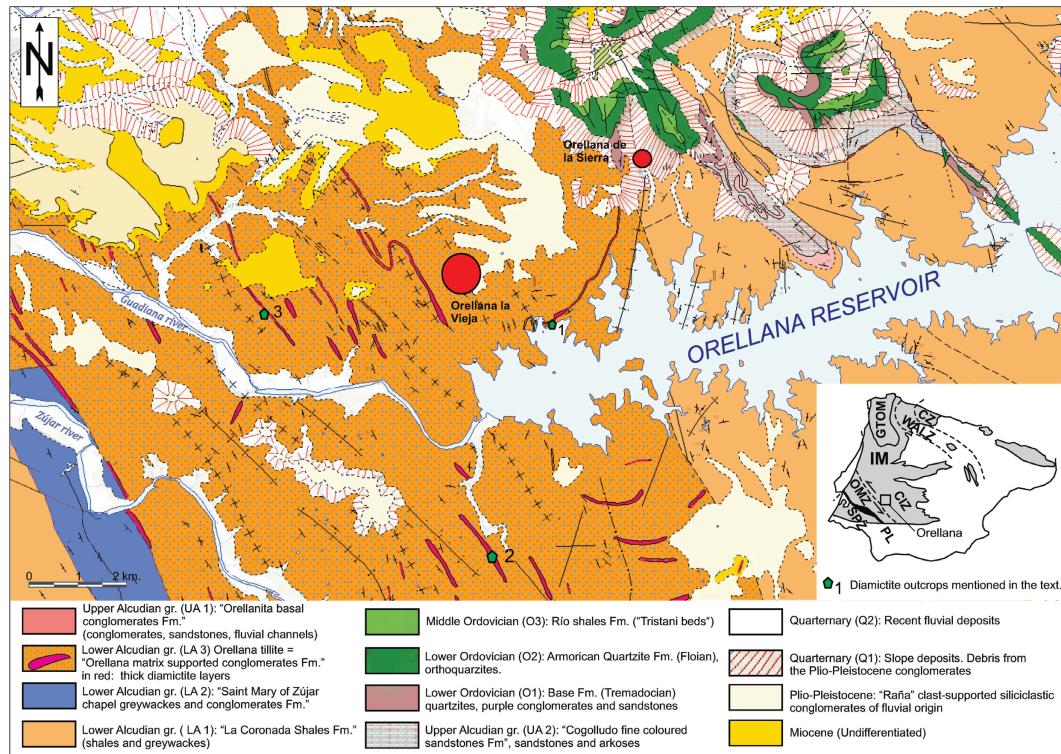

Figure 3.—Geological map of part of the Alcudia Antiform at the Orellana reservoir (Orellana region, Central Iberian Zone; from Linnemann *et al*., 2018 and references therein) . Locality 1 (stop 3): waterline of the sweet-water reservoir (images see Fig. 5), N 39°00'8.4"; W5°31'18.9". Locality 2 (stop 4): roadcut near Orellana (images see Fig. 4), N 38°52'52.8"; W5°29'5.6". Locality 3: roadcut near Orellana, sample location of OR-1 (images see Fig. 5), N 39°00'4.6"; W5°34'11.9". Red dots are towns. Inset map: CIZ- Central Iberian; CZ-Cantabrian, GTOM- Galicia-Tras os Montes, MZ – Moldanubian, OMZ- Ossa Morena, PL- Pulo do Lobo and SPZ- South Portuguese Zones.
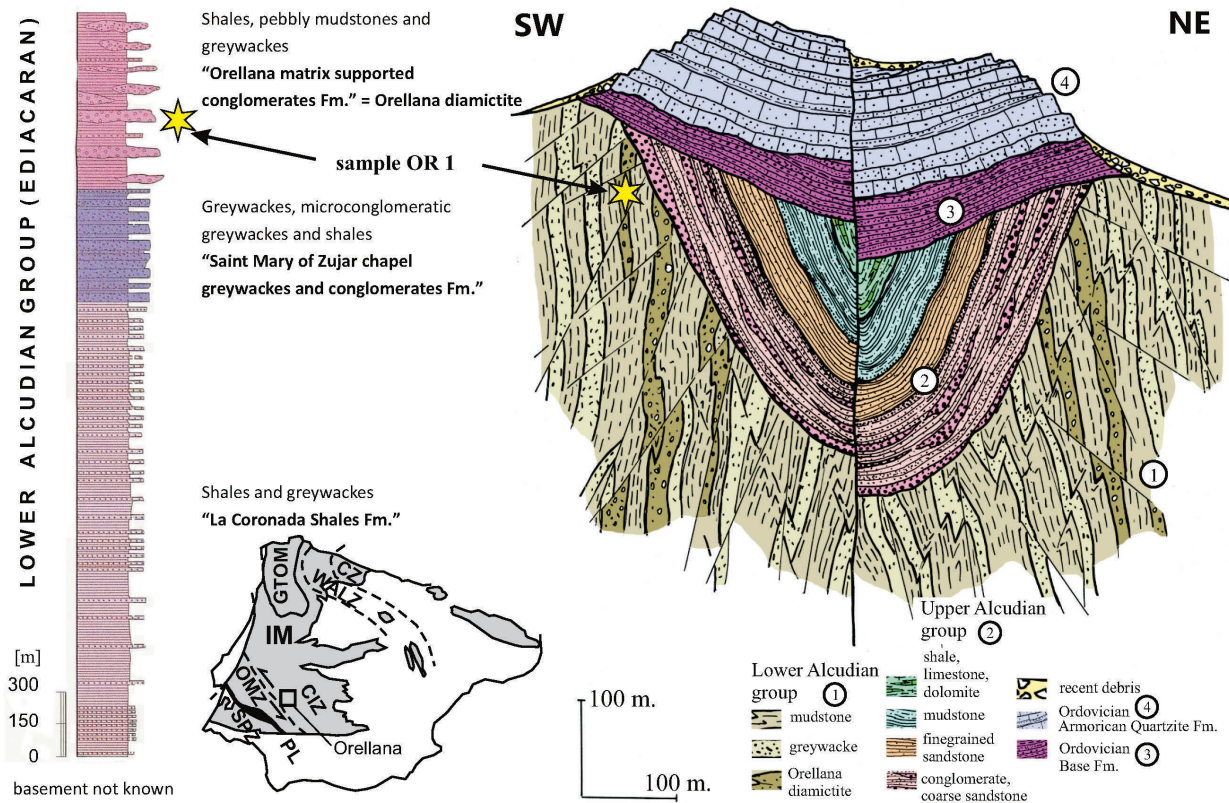
Figure 4.—Idealized section of the Lower Alcudian-Domo Extremeño Supergroup and overlying Ordovician strata from the Alcudia Antiform near Orellana (Central Iberian Zone, Spain). Left: stratigraphic log of the "Lower Alcudian" part; from García Hidalgo *et al.*, 1993; Pieren, 2000); for abbreviations of inset, see Fig. 2.

dropstones (Fig. 5B), rain-out sediments (Fig. 5C), flat iron shaped pebbles ("Bügeleisen-Geschiebe"; Fig. 5D), and facetted pebbles (Fig. 5E). Pebble size varies between a few millimetres and 20 cm. Glaciomarine diamictite occurs in ca. 10 to 50 m thick beds in the region of Orellana la Vieja, Orellana de la Sierra and the Orellana dam (Pieren, 2000).

U-Pb ages of detrital zircons are represented in figure 6. Because ash beds and fossils have not been found in the investigated sections, the maximum depositional age (MDA) had to be used for the stratigraphic age determination (Condon & Bowring, 2011).

The maximum depositional age for each sample was calculated from the youngest zircon population for each sandstone sample (Fig. 6). The zircons from the Orellana diamictite (sample OR1) in the Lower Alcudian-Domo Extremeño Supergroup of the Central Iberian zone yielded a maximum depositional age of 565 ± 4 Ma (Fig. 6) (Linnemann *et al*., 2018). The maximum depositional age

for the diamictites is significantly younger than that for the Gaskiers glaciation in Newfoundland. Thus, the diamictite should represent a post-Gaskiers glacial event during Ediacaran time. Alternatively, a shifting of the ice center from Avalonia (Gaskiers glaciation, ca. 579-581 Ma) to West African peri-Gondwana (Weesenstein-Orellana glaciation, ca. 565 Ma) over time would be possible. The detrital zircon populations of the Weesenstein-Orellana glaciation support a palaeoposition marginal to West Africa (Linnemann *et al*., 2018).

Age constraints completely rule out a correlation of this glacial event recorded in the Cadomian metasedimentary rocks with the Gaskiers glaciation, which occurred around 579-581 Ma (Bowring *et al*., 2002, Thompson *et al*., 2014; Pu *et al*., 2016). Instead, a correlation with a glacial event recorded in Northwest Africa (Morocco) (Vernhet *et al*., 2012) and in Arabia (Vickers-Rich *et al*., 2012) is much more realistic and provides information about the timing of this young Neoproterozoic glacial
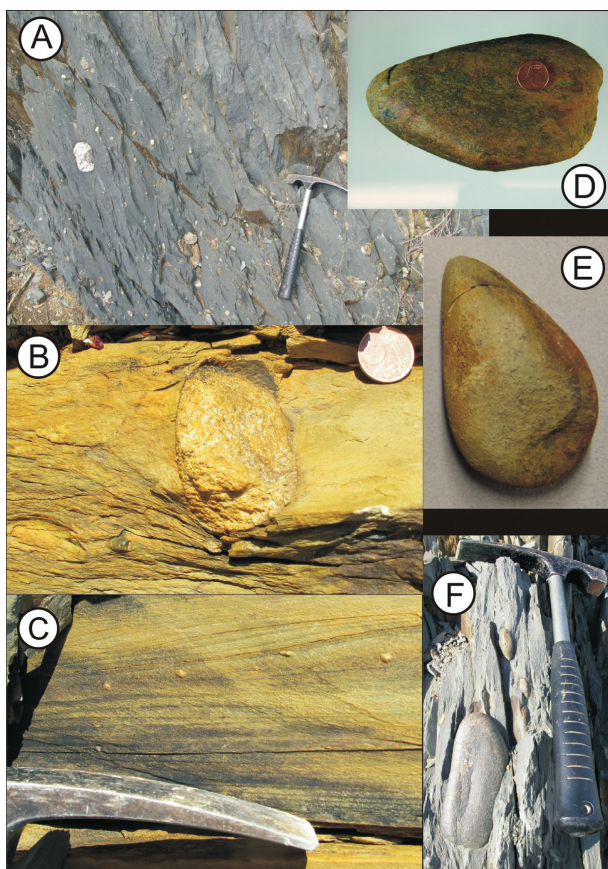
Figure 5.—Images from the glaciomarine deposits of the Orellana diamictite, Alcudia Antiform, Central Iberian zone, Spain. A. Diamictite containing pebbles of sedimentary rocks (quartzite, greywacke) (Locality 2, Fig. 3). B. Dropstone in a rainout deposit. C. Rainout deposit with millimetre-sized rock fragments. D. Faceted and flat iron shaped pebble in a rainout deposit (flat faceted top and sharp left end formed by ice abrasion; stump right end formed in the pressure shadow during ice abrasion ("Bügeleisen-Geschiebe") (Locality 3, Fig. 3). E. Facetted pebble from a rainout deposit (flat iron-shaped pebble = "Bügeleisen-Geschiebe") (Locality 3, Fig. 3). F. Large flat iron-shaped pebble (= "Bügeleisen-Geschiebe") a fine-grained diamictite matrix; B, C and F images photographed in a roadcut at Casa el Canchal (N 38°52'52.8"; W5°29'5.6").

event. At Bou Azzer (Moroccan Anti-Atlas) Vernhet *et al.* (2012) describe glaciomarine structures (striated pavement on rhyolites) within the Ouarzazate group. The age of the latter is constrained by published U-Pb ages of the Ouarzazate Supergroup and can be placed in a time window between ca. 570 and 562 Ma (Karaoui *et al.*, 2015). In Arabia, another glaciomarine diamictite has been detected in Ediacaran sedimentary deposits of the Dhaiqa formation. An ash bed just below the diamictite provided a U-Pb

age of 560±4 Ma (Vickers-Rich *et al.*, 2012). Further, an Ediacaran glacial deposit (Moelv diamictite) crops out in Baltica (Bingen *et al.*, 2005). But available age data are not sufficient to constrain an age younger than the Gaskiers glaciation (Bingen *et al.*, 2005). Existence of this Cadomian glaciation could be the reason for the negative excursion of the $\delta^{13}C$ curve (Shuram-Wonoka anomaly) (Halverson *et al.*, 2005: fig. 18) (Fig. 7). The origin of the Shuram-Wonoka anomaly is still under discussion. In addition to all, Letsch *et al.* (2018) reported also equivalents of the true Gaskiers glaciation in a time window in the range of 592 to 579 Ma from the Anti-Atlas (Morocco). It seems that West Africa and adjoining terranes represents an area that was affected by several glacial events in Upper Ediacaran time.

October 22: Plunging into reefal worlds, Villarta Formation

Drive to Stop 5. The picturesque village of Villarta de los Montes (province of Badajoz) is located in a hilly area, on the foothills of the Umbria Mountains. Its setting is quite far from other towns of the area, from which it is separated by a rugged orography of enormous magnificence and scenic beauty, covered with forests and scrubland. Villarta "of the mountains" is famous for the hunting parties that are organized in the Cíjara Regional Hunting Reserve, and the fishing activities that take place in the neighbouring Cíjara dam. The northern shore of the dam has represented, for decades, the target of Ediacaran palaeontological research: along a W-E transect of about 4 km, the hills offer some key exposures of the Castañar and Villarta formations. The latter are unconformably overlain by the Lower Ordovician "Purple Series" and Armorican Quartzite, which form the mountainous crests.

STOP 5. Visiting the Hermitage of Santa María de la Antigua

On the mountainous heights, after overpassing the bridge that cross the Cíjara reservoir, stands the hermitage of "Nuestra Señora de la Antigua" (Our Lady the Old), protector of Villarta de los Montes. The basement of the hermitage is the stratotype of the so-called La Antigua Conglomerate Member (Castañar Formation). The unit, up to 100 m thick, consists of clast-supported heterolithic granule-to-cobble clasts embedded in an
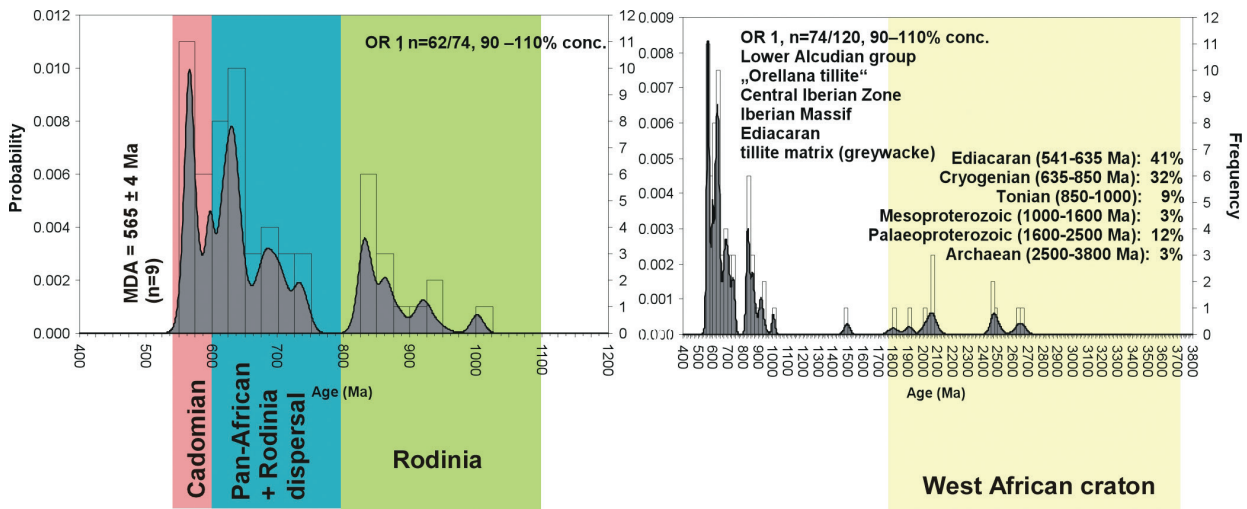
Figure 6.—Combined binned frequency and probability density distribution plots of U-Pb LA-ICP-MS ages of detrital zircon grains from the Lower Alcudian-Domo Extremeño Supergroup (Ediacaran) in the ranges of 400 to 1200 Ma (left) and 400 to 3800 Ma (right): OR1 (greywacke, diamictite matrix, Ediacaran, Orellana diamictite, Central Iberian Zone, Spain).
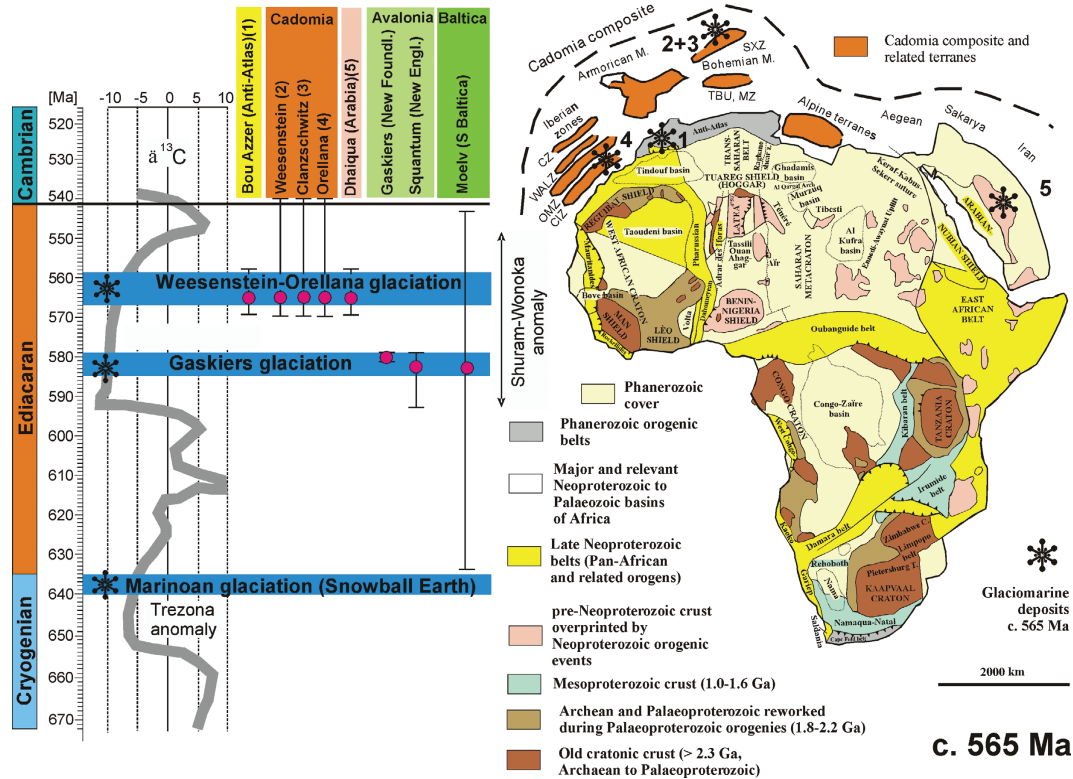

Figure 7.—Timing of the Weesenstein-Orellana glaciation and its relation to the δ^{13}C curve (Halverson *et al.*, 2005) (left), palinspastic map showing palaeopositions of Ediacaran post-Gaskiers glacial deposits in peri-Gondwana, North Africa, and Arabia (right). Cadomia composite includes the different terranes of the Cadomian orogen distributed now in Western and Central Europe (peri-Gondwanan West Africa); modified from Linnemann *et al.* (2018).
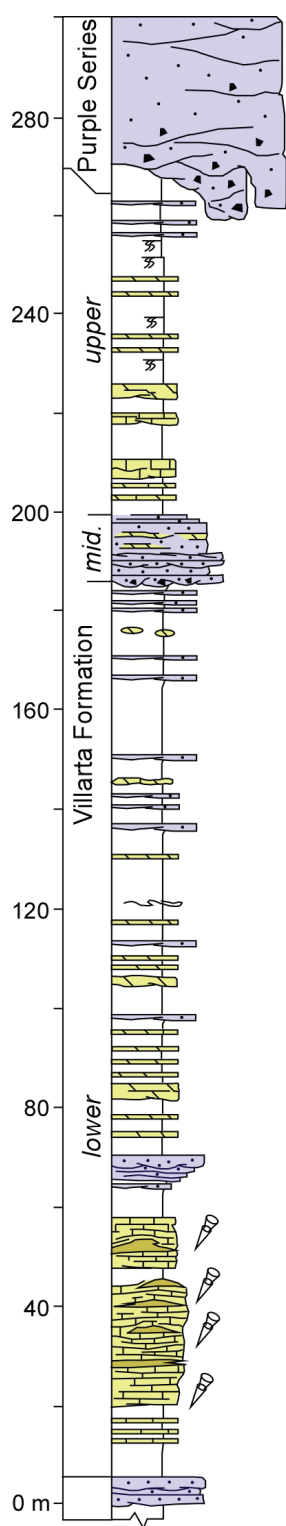
Figure 8.—Stratigraphic log of La Majada del Andaluz stratotype, with complete lower and middle members of the Villarta Formation; cones represent *Cloudina*-bearing buildups; carbonate in yellow, conglomerate and sandstone in purple, and shale in white; upper member with burrowing symbols.

unsorted coarse- to fine-grained litharenite matrix. Clasts are composed of greywacke, sandstone, shale, chert and vein quartz. The member unconformably overlies the Lower Alcudian-Domo Extremeño greywackes.

STOP 6. Sequence analysis of Cloudina-microbial reefs

Following a pathway that follows the northern shore of the Cíjara dam, we will enter a private area for livestock farming. A sheep, pig and cattle farm, known as "la Majada del Andaluz" (the Andalusian sheepfold), marks the beginning of this private pastureland. We advise against any furtive sampling of rocks: if you want to visit the area on your own, please, request permission at the town hall before entering this private area.

The "Majada" lies at the mid-point of a stratigraphic log that begins at the Cíjara dam and reaches the overlying Lower-Ordovician "Purple Series" on the crest of the hill: the stratotype of the Villarta Formation. The latter displays three distinct members: (i) an alternation of lenticular and bedded carbonates embedded in greenish shales (Figs. 8, 9A-D); (ii) a sandstone-dominant unit passing upward to sandy dolostones (Fig. 9E-F); and (iii) an alternation of shales and bedded carbonates (Fig. 9G-H).

Stop 6 represents the stratotype of the formation (GPS: N39º13'52.86'', W39º13'52.86''), where complete lower and middle members are well exposed (Fig. 8). The lower member consists of a superposition of shale-marlstone-limestone cycles, up to 2.4 m thick. The uppermost part of each cycle is marked by *Cloudina*-microbial patch-reefs and/or biostromes, dominated by thromboid textures and punctuated by *Cloudina* shells preserved both upright and lying on the surface. *Cloudina*-thromboid-stromatoid buildups have yielded, after acid etching, specimens of *Cloudina* (*C. carinata*, *C. hartmanae* and probably *C. xuanjiangpingensis*), *Sinotubulites* (*S. baimatuoensis*) and *Protolagena* sp. (a problematic flask-shaped microfossil; Cortijo *et al*., 2010, 2015). The heterolithic middle member consists of conglomerate, sandstone and shale beds. Sandy litharenites show common trough cross-stratification sets punctuated by channels. Finally, the upper member comprises limestone/shale alternations, the latter with trace fossils of an appearance consistent with a Cambrian age (Álvaro *et al*., 2019).
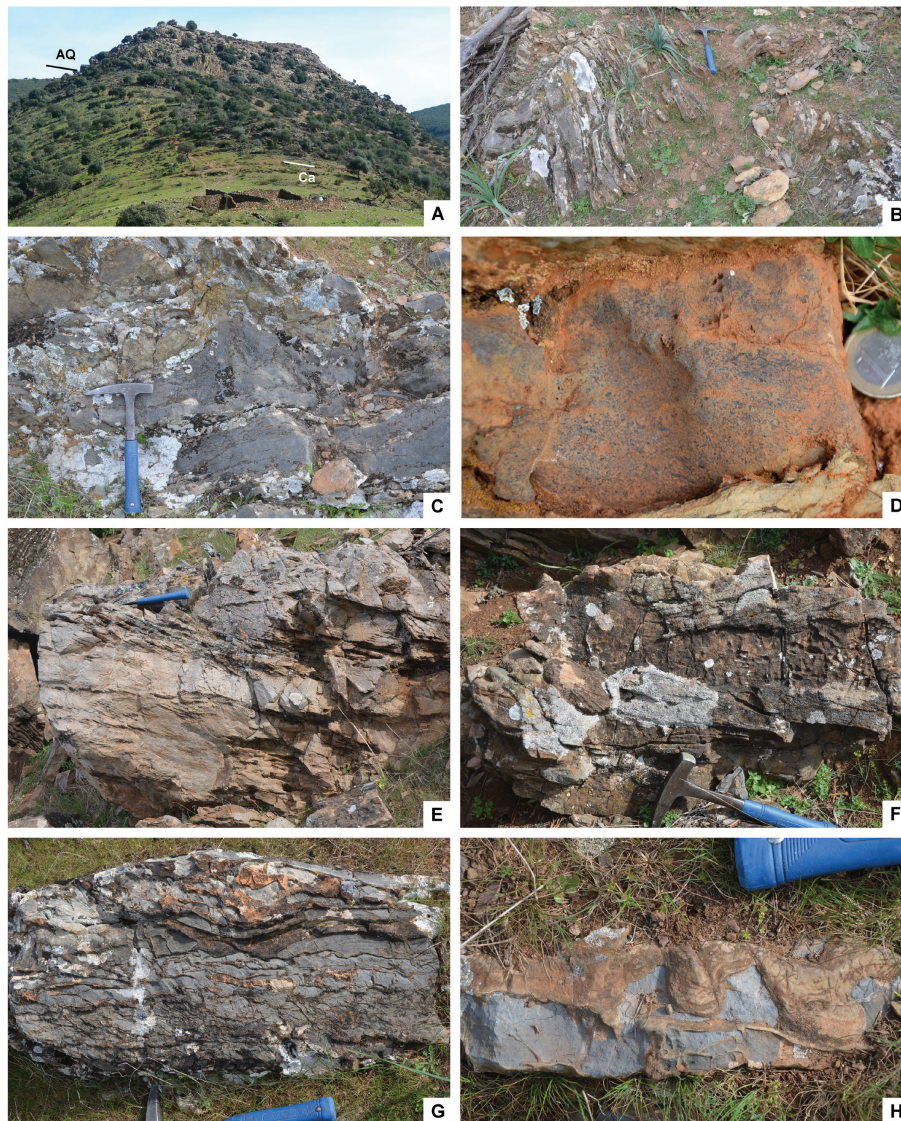
Figure 9.—Field aspect of the Villarta Formation at stratotype. A. "Majada del Andaluz" section seen from the farm unconformably overlain by the Lower-Ordovician "Purple Series" that forms the crest of the hill; Ca- Castañar Formation, AQ- Armorican Quartzite (Purple Series Member) Formation. B. Slumped limestone/shale alternations; lower member. C. Patch-reef surrounded by bedded flanks; lower member. D. Core reef rich in autochthonous and parautochthonous shells encased in a thromboid mass. E. Superposed trough cross-stratification sets displaying grading from basal conglomerate (lag) to upper coarse- to medium-grained litharenites; middle member. F. Interbedded channels with subrounded granule clasts crosscutting sandy shoals; middle member. G. Superposed centimetre-thick limestone layers punctuated with wavy and stylolytized contacts; orange colours reflect dolomitization; upper member. H. Load casts of brownish silty dolostone on blueish limestone; upper member.

STOP 7. Geometrical relationships of Cloudina-microbial reef complexes

This stop is located some 500 m SE of stop 6. Frame reefs display two main geometries, core and flank beds, which stand out in contrast as lenticular and bedded masses of beige resistant limestones encased in thinly bedded, greenish shales and marlstones (inter-reef sediments; Fig. 10A-B). The core geometry ranges from patches or isolated pillow-shaped masses up to 0.8 m thick, to bioherms or lenticular masses of larger dimensions, less than 1.8 m thick, where well-developed flank beds commonly intercalate with inter-reef sediments. Locally, these individual geometries are arranged into stacked patches becoming both vertically and laterally aggregated into reef complexes, up to 2.8 m high and 6 m wide.

Texturally, the reef-core facies consists of *Cloudina*-thromboid boundstones and floatstones with local development of peloidal and intraclastic pockets, punctuated by domal stromatolites. Due to intense neomorphism, the calcified microbial communities are heterogeneously preserved, with clotted textures occurring directly encrusting both microsparitic substrates and shelly walls. The microbial framestone is dominated by clotted, peloidal, fenestral textures, and subsidiary stromatolitic microsparite/sparry textures.

Flank beds form the margin of some bioherms and reef complexes. Proximal flanks consist of well-bedded, intraclastic packstone-to-wackestone and nodular limestones rich in breccia intraclasts and oncoidal lags. Proximal flanks grade laterally into thinly bedded (0.1-0.2 m) limestones and marlstones that finally alternate with shales bearing centimetre-thick nodules (inter-reef sediments). Flank beds thin away from the core passing laterally into debris beds or flat bedded inter-reef sediments. Inter- and off-reef sediments are dominated by bedded marlstones and shales. Some flanks are slumped and contain reef blocks and slope intraclast beds (Fig. 10D). Inter-reef, thinly laminated shales and marlstones display contorted and convolute folds (laterally extensive series of folds confined between two undeformed layers) and slumps bearing scattered shells preserved as moulds. Larger bioherms and reef complexes contain Neptunian dykes (Fig. 10C), up to 30 cm in width. These were infilled with angular calcite and dolomite clasts, up to 5 cm long, embedded in a microsparitic matrix with both calcite and dolomite cements.

STOP 8. When reefs nucleated along the border of an unstable block

In the easternmost outcrops of the visited W-E transect along the northern shore of the Cíjara dam, the lower member consists of carbonate/shale alternations. Carbonates, up to 1.4 m thick, display lower shelly-microbial frame-building textures commonly scoured by upper chaotic breccias (Fig. 10E-G). The latter, up to 30 cm thick, are unsorted, polymictic and rich in angular to subrounded, pebble- to sand-sized clasts. Evidence of rebrecciation is observed as larger angular clasts are composed of polyphase breccia generations. In contrast, smaller clasts exhibit some degree of rounding and sorting. The breccia is dominantly clast-supported, with a matrix rich in illite locally punctuated with framboidal pyrite. Polymictic

clasts consist of clotted limestone and partly or wholly dolomitized limestone, and subsidiary shale, chert and phosphate. Steeply dipping fissures and veins occur crosscutting the carbonate beds and their clast counterparts. Veining, associated with hematite and barite precipitation, is conspicuous both in the encasing limestone and clasts. Some fissured breccia lags are sealed by patch-reefs, up to 60 cm high and 80 cm in basal diameter, which have no distinct flanks. This outcrop represents the easternmost exposure of the Villarta Formation in the area. To the east, the Navalpino megabreccia Bed unconformably overlies the Castañar Formation (the latter known as the "Torilejo conglomerates" in regional geology).

October 23: Traditional outcrops since the 1970s

During this excursion will be examined several sections in the area of La Nava de Ricomalillo, Toledo Province, which are of both historical and contemporary interest for questions on the Ediacaran-Cambrian transition in the Central Iberian Zone. Sections west of La Nava de Ricomalillo provide some of the most important outcrops of the Cíjara and Pusa formations. An uncompleted railway trench that runs approximately in a S-to-N orientation provides exposures of the Cíjara and Pusa formations, which it cuts obliquely. This track, which is now "Vía Verde", a recreational "green" path, runs close to the Huso (or Uso) river, also provides important outcrops. Additional sections are found in road cuts. Three stops will be visited during this field trip (Fig. 11).

STOP 9. Denudation of a Cadomian Arc along the Cubilar stream

Location.- The section is located along the Arroyo de Cubilar stream which can be accessed by dropping down from road TO-1195 about 6.5 km from La Nava de Ricomalillo. This section exposes the lower part of the Pusa Formation, the Fuentes megabreccia Bed and the Cíjara Formation, including good exposures of channelized conglomerates in the latter.

Description. The first part of the section shows intermittent outcrop continuity of the lower part of the Pusa Formation. Trace fossils are present, but hard to find, in the first slope including *Treptichnus* isp. (Jensen *et al.*, 2007: fig. 2a, f). The Fuentes megabreccia is reached after a 20 minutes' walk during which intermittent outcrop, showing
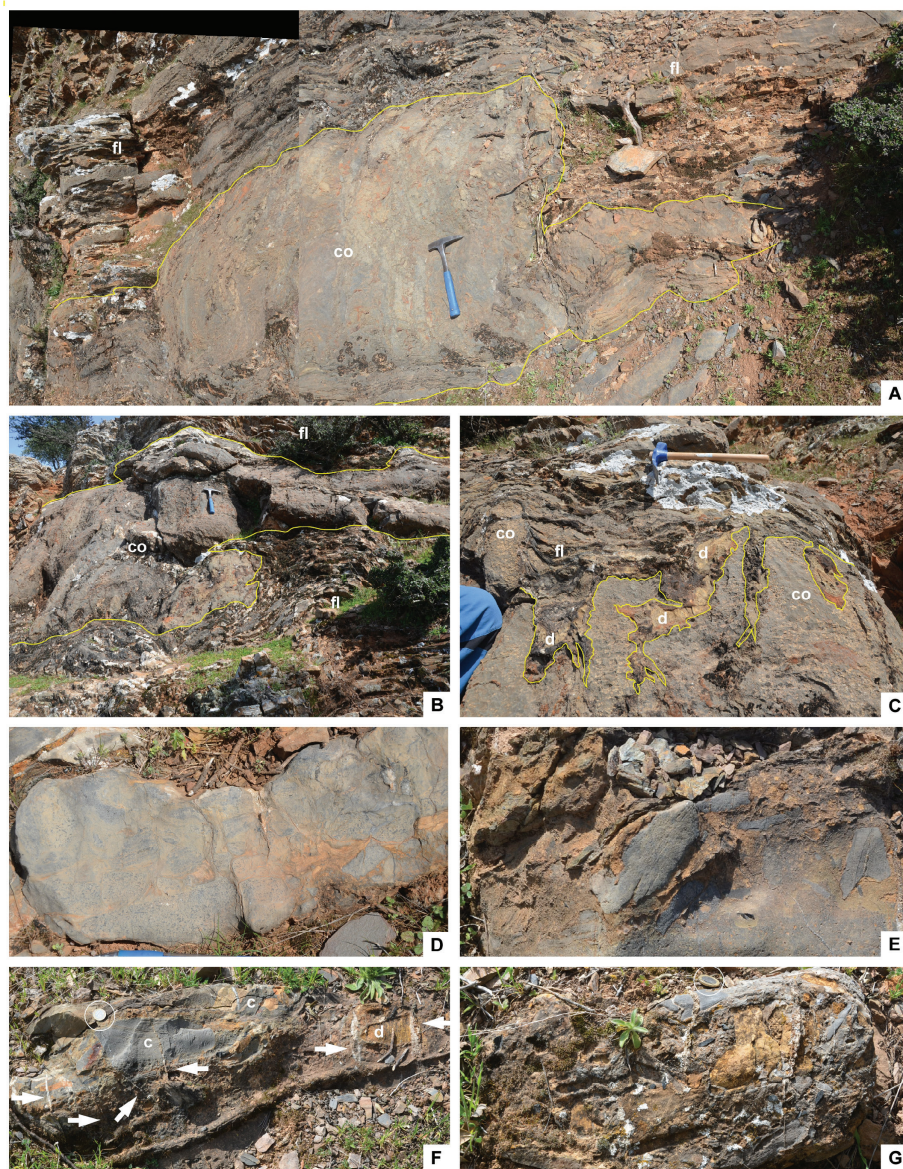
Figure 10.—Field aspect of the cloudinid-bearing limestones from the lower member of the Villarta Formation along a W-E trending, ca. 3 km transect along the northern shore of the Cíjara dam. A. Massive cloudinid-thromboid core (outlines in yellow) surrounded by bedded flanks. B. Superposed patch-reefs forming a reefal complex surrounded by flanks. C. Neptunian dykes marking the top of a reefal core, infilled with reefal intraclasts and occluded with sparry mosaics of dolomite, overlain by a verticalized patch-reef surrounded by flanks. D. Nodular to brecciated aspect of a flank. E-G. Slope-related clast-supported breccia with angular limestone and dolostone clasts, calcarenite matrix and dolomite cements hosting a network of unoriented veins (arrowed) crosscutting clasts and/or matrix; c- blueish calcite, Co- core; d- orange dolomite, fl- flank.

typical examples of laminated siltstone and fine sandstone of the Pusa Formation are exposed. At outcrop scale, the Fuentes megabreccia Bed is composed of two principal levels separated by laminated sandstone (Fig. 12A). Outcrops on the NE side of the same hill show clearly the channelized nature of the megabreccia lobes (Fig. 13). The breccia contains a variety of clasts including greywacke, shale and carbonate clasts (Fig. 12C). Carbonate blocks in the lower interval have yielded examples of silicified *Cloudina* shells. The material is typically poorly preserved (Fig. 12B), but clear examples of *Cloudina carinata* have been encountered. Following Arroyo de Cubilar
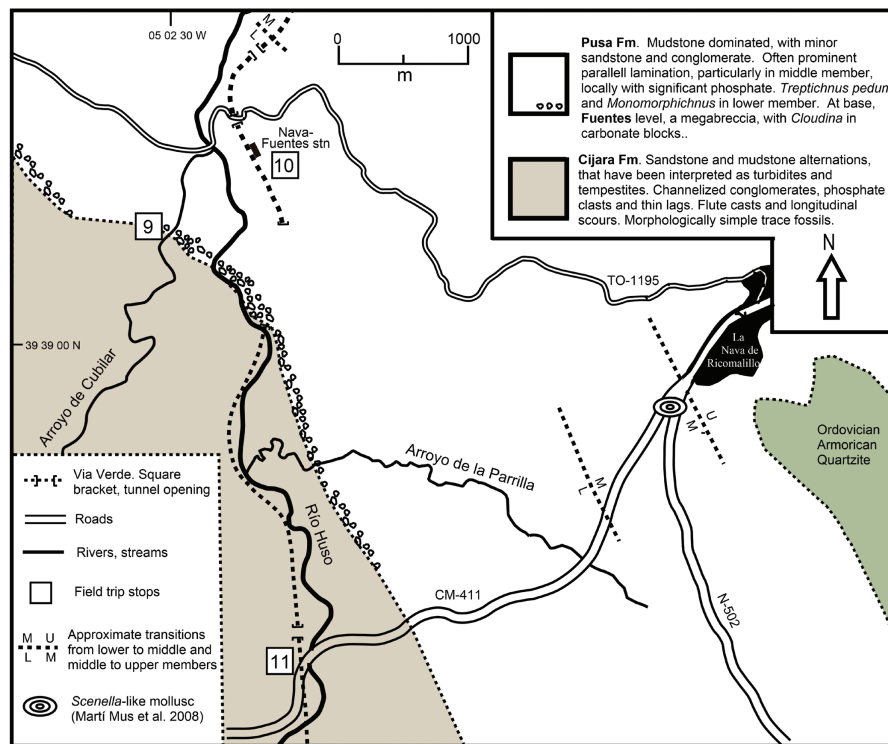
Figure 11.—Location map for stops 9, 10 and 11 in the area of La Nava de Ricomalillo.
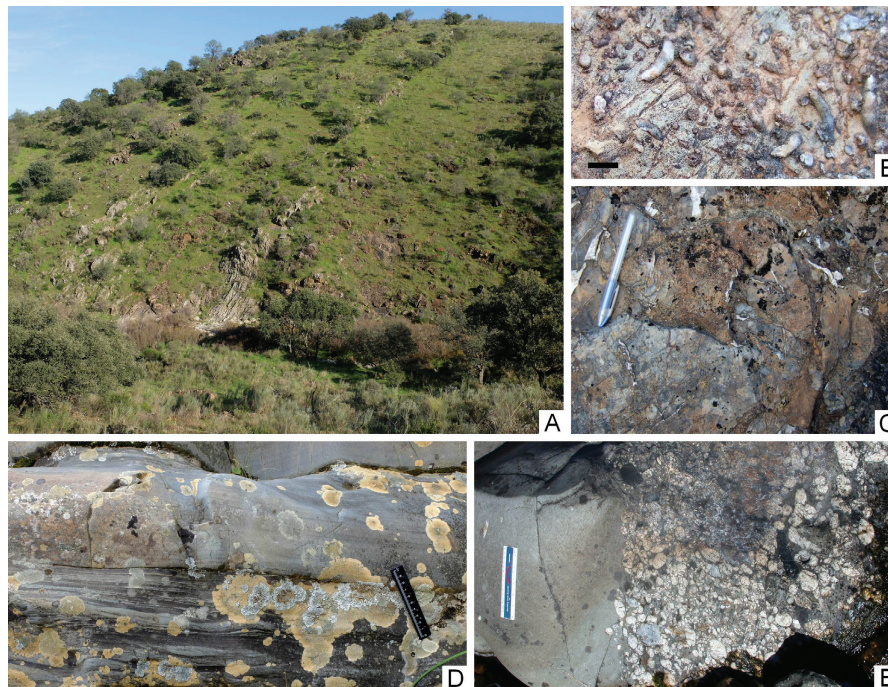

Figure 12.—Fuentes megabreccia Bed and Cíjara Formation in Arroyo de Cubilar. A. Outcrop image of the Fuentes megabreccia. Several channelized intervals separated by lighter coloured sandstone are seen. B. Silicified *Cloudina*; scale bar = 2 mm. C. *Cloudina*-bearing carbonate block in the Fuentes megabreccia. D. Example of typical bedding in the Cíjara Formation. Background shale beds punctuated with siltstone and sandstone interbeds displaying scouring bases, low-angle to cross-laminated sets, ripple tops and flaser-to-lenticular laminae. E. Base of polymictic conglomerate channel rich in hydrothermal quartz granules; top to the right.

in a southerly direction, sandstone and minor mudstone beds of the Cíjara Formation are seen (Fig. 12D). Polarity is opposite to that of the Pusa Formation, and the contact here between the Cíjara Formation and the Fuentes megabreccia is faulted. Sandstone beds often show graded bedding and ripples. After a further 10 minutes' walk, channelized conglomerates with abundant hydrothermal quartz clasts are encountered (Fig. 12E). The conglomerates are mainly clast-supported but other levels further along the Arroyo Cubilar are matrix-supported. Other sedimentary structures in the Cíjara Formation include flute, tool and frondescent marks.

STOP 10. Historical Ediacaran-Cambrian boundary reference section along an abandoned railway line

Location. This stop is reached by entering a dirt road that leads off road TO-1195, some 6 km from La Nava de Ricomalillo.

Description. Outcrop along the abandoned railtrack in both directions from the derelict Nava-Fuentes station house exposes portions of the lower member of the Pusa Formation. This is dominated by clayey sediments with minor sandstone interbeds, which has been interpreted as deposited in an offshore-dominant setting. Outcrop on either side of the station house have been given as being about 250 m above the base of the lower member. This is the principal section from which trace fossils were described from the lower part of the Pusa Formation by Brasier *et al.* (1979), Palacios Medrano (1989) and Vidal *et al.* (1994). Bedding dips steeply and a peculiarity of the succession is that trace fossils are generally seen only

on upper bedding surfaces whereas bed bases are barren. Bedding is normal in this part of the section and observation will be made on the western face of the track. During this field trip observations will concentrate on two stretches of outcrop (Fig. 14).

Beltanelliformis level. An outcrop some 250 m SE from the station building contains upper bedding surfaces with densely packed organic fossils, now elongate but almost certainly originally circular (Fig 14A). These have been referred in the literature to as *Chuaria*, *Beltanelloides* and *Beltanelliformis*. The outcrop has become degraded by natural collapse but also by the activity of collectors. There are reasons to believe that these occurrences originally covered several square metres. Trace fossils have not been recovered from this part of the section, but very rare filaments have been found.

Cambrian-type ichnofossils. Passing the station houses in a NW direction, outcrops on the left hand side after passing a short tunnel, contain surfaces with abundant trace fossils (Fig. 15A). Most common are horizontal simple millimetric to sub-millimetric trace fossils of *Helmimthoidichnites* type. Also seen are larger irregularly winding horizontal forms. Favourable light conditions are essential for a good view of these trace fossils. A short distance further north, more complex trace fossils are seen: these include examples of *Treptichnus pedum* (Fig. 15B-C) and probes (Fig. 15D). Faintly developed *Monomorphichnus* have also been observed.

Discussion. In several publications, the transition between the two aforementioned sections has been suggested to represent the Precambrian-Cambrian boundary interval and proposed as a regional Ediacaran-Cambrian transition reference section and the base of the regional

Figure 13.—Fuentes megabreccia Bed as seen from the Huso river, with superposition of four (*a* to *d*) slope-related breccia aprons, overlain by the Pusa Formation (right); arrows mark sliding movement.
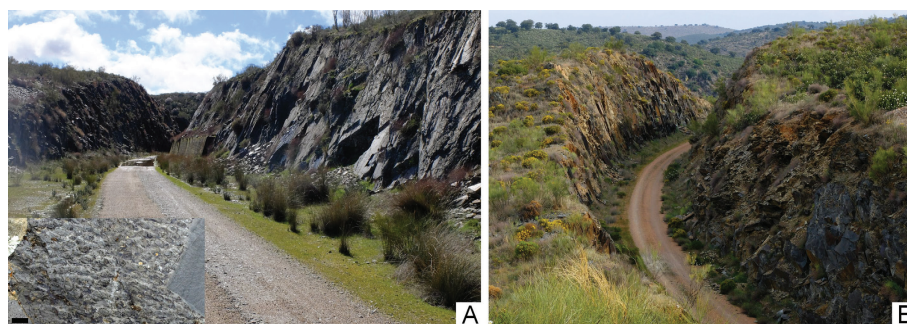
Figure 14.—Outcrop of lower member Pusa Formation along Via Verde abandoned railtrack section. A. Part of section with *Beltanelliformis* (inset) traditionally interpreted as Ediacaran in age. B. Part of section with Cambrian-type trace fossils.
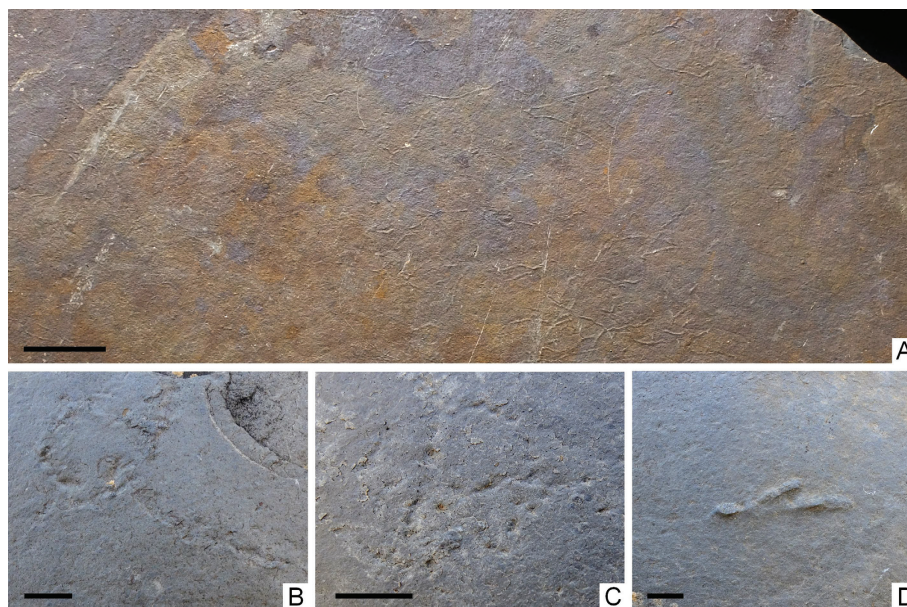

Figure 15.—Trace fossils from the lower member of the Pusa Formation; all views are of bed tops. A. Dense cover of *Helminthoidichnites*-type trace fossils and a larger meandering form (? *Helminthopsis*); scale bar = 50 mm. B-C. *Treptichnus pedum*. D. Unidentified trace fossil consisting of apparently connected vertical hook-shaped probes; scale bars in B to D = 10 mm.

Cordub(i)an Stage (e.g. Liñán *et al*., 1993, 2002; Gámez Vintaned, 1996; Gámez Vintaned & Liñán, 1996, 2007; for a critical reappraisal, see Álvaro *et al*., 2019). It is, however, likely that the succession of strata observed here are younger than the currently used age for the base of the Cambrian at about 539 Ma. *Treptichnus* and *Monomorphichnus* have been recorded (Brasier *et al*., 1979; Jensen *et al*., 2007) from a nearby location that probably is at a lower stratigraphic level. The Fuentes megabreccia contains allochthonous *Cloudina* shells, including *Cloudina carinata*, suggesting a late Ediacaran age for the involved carbonate blocks, encased in a younger megabreccia bed. As a result, the pre-Cordub(i)an part of the Pusa Formation, underlying the lowest record of *Treptichnus*, should be Terreneuvian in age. Some support for this comes from a detrital zircon date of 533 Ma recorded by Talavera *et al*. (2012) from the middle portion of the lower Pusa Member from a nearby section. More precise radiometric dating is needed to confirm this age.

STOP 11. Simple trace fossils from the Cíjara Formation

Location. Road cut along road CM-411, at 39°37'36"N, 05°01' 45"W. IMPORTANT: this is a regularly trafficked road with speed limit of 90 km/h. Take care when crossing and avoid entering pavement.

Descripton. The road cut on the eastern side contains several surfaces of overturned Cíjara Formation strata (Fig. 16A) with several bed soles showing simple trace fossils typical of the Cíjara Formation (Fig. 16B). Trace fossils from this outcrop have been figured in Jensen *et al.* (2007: fig. 2e) and Jensen & Palacios (2016: fig. 3e). The western road cut shows channelized conglomerates containing phosphate clasts. Also note well-developed folds typical for the upper part of the Cíjara Formation in this area.

Some 200 m north along Vía Verde, a bed sole contains a structure consisting of two apparently joined sets of paired ridges or lobes (Fig. 16C). This shows resemblance to bilobed trace fossils, which, with a width of some 15 mm, would be unusually large for a late Ediacaran trace fossil. As this is the only known occurrence of this type of structure in the Cíjara Formation, its interpretation is better left open.

October 24: Treasures hidden under the Tagus river

Several sections of the Tagus river are dammed along Spain and Portugal. Upstream of the Almaraz nuclear power plant, the Valdemoreno and Valdecañas reservoirs attempt to maintain the river's flow during the months of drought. The mouth of the waters that cool the nuclear reactors of the Almaraz plant marks the beginning of García Hidalgo's (1985) Arrocampo log. Along the following 2 km on the right bank, the log represents what is here proposed as the "ichnological" Ediacaran-Cambrian boundary stratotype of the Iberian Massif. This ribbon exposure is only accessible when the upstream reservoirs are closed: between September and March. Outside those months, the outcrops are partly covered by water and the visit is discouraged.

STOP 12. The "ichnological" Ediacaran-Cambrian boundary stratotype

Due to the influence of the Cadomian orogen, the denudation of uplifting Arc areas led to deposition of coarse-grained siliciclastic sediments infilling the back-arc basin that we know now as the Central Iberian Zone (Álvaro *et al.*, 2019). The poisoning effect on carbonate factories of this stepwise denudation was coeval with the breakdown of the back-arc basin into uplifting, rotating and collapsing platform-blocks. As a result, each block recorded diachronous processes of carbonate production and terrigenous input. The limits of the Villarta Formation are not isochronous throughout the visited stops, and the members defined in its stratotype (Villarta de los Montes) cannot be easily followed laterally.

This is the case of the Arrocampo log. This carbonate-dominant succession is here interpreted to represent the upper member of the Villarta Formation, whereas the lower member, rich in *Cloudina*-bearing limestones, is poorly preserved here. The upper member of the Villarta Formation shows, in ascending order, a succession of trough cross-bedding sets and beds with low-angle to parallel laminae, locally punctuated with centimetre-thick stromatolites (Fig. 17A-D) and possible *Beltanelliformis* moulds (Fig. 17E) A distinct level marks a sharp difference in environmental conditions; it is characterized by the presence of herringbone cross-laminated beds
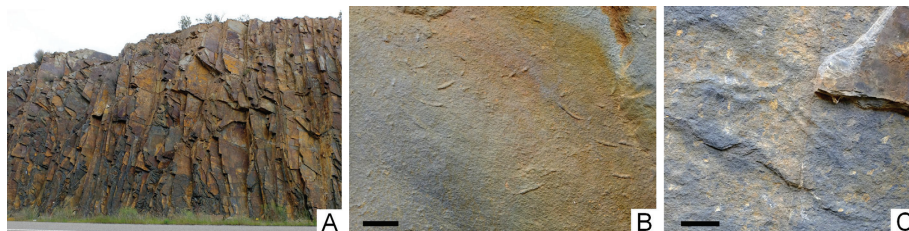

Figure 16.—Cíjara Formation. A. Aspect of outcrop along road CM-411. B. Simple trace fossils on bed sole. The trace fossils have been eroded but an irregular meandering habit is indicated. C. Problematic paired bed sole structure in section along Vía Verde; scale bar = 30 mm.

(Fig. 17F) unconformably overlain by a decimetric breccia bed related to platform-block breakdown (Fig. 17G). The uppermost part of the member displays, centimetre- to decimetre-thick, bedded to wavy strata (Fig. 17H). The member consists of impure limestones due to the conspicuous presence of silty grains of quartz and feldspar, which reflect the episodic influence of an actively denudating Cadomian Arc situated to the SW.

The Villarta Formation is conformable overlain by a monotonous shaly succession, which represents the stratotype of the Arrocampo Formation (Álvaro *et al.*, 2019). The stratotype is a shale-dominated unit with subsidiary
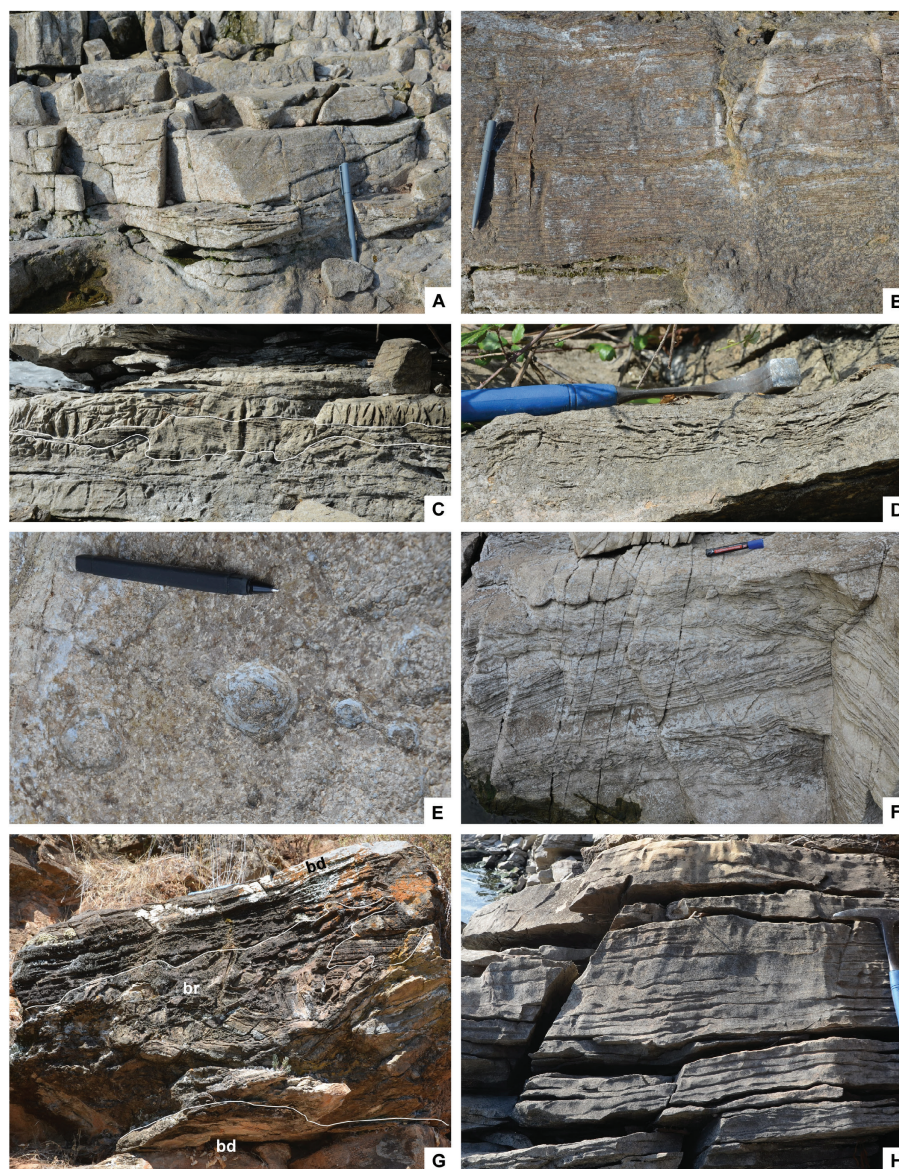

Figure 17.—Field aspects of the upper member of the Villarta Formation along the Arrocampo log. A. Centimetre-scale channel with axis perpendicular to the image, overlain by a superposition of trough cross-laminated sets. B. Finely parallel to low-angle laminated limestone. C. Scouring surfaces (outlined in white) separating trough cross-laminated sets. D. Crinkled stromatolites with fenestral porosity reflecting episodic development of microbial mats. E. Upper surface of a bed exhibiting hemispheroids with concentric ridges mimicking *Beltanelliformis*. F. Herringbone cross-laminated beds underlying the breccia bed of next picture. G. Slope-apron breccia lens (br) with intraclastic granules and boulders embedded (white lines) in normal bedded strata (bd). H. Uppermost part of the member showing thinly bedded limestones with slightly wavy-to-rippled tops.

Figure 18.—Arrocampo Formation in the Tagus river area west of Almaraz. A. Trace fossil-bearing bed surface along Tagus the river of thin-bedded sandstone and shale alternations with prominent rippled bed tops. B. *Treptichnus pedum* on bed sole from Tagus river section; coin for scale is 19 mm. C. *Treptichnus pedum* on bed sole from section of Arrocampo Formation along road A5/E90; scale = 5 mm

sandstone interbeds (Fig. 18A) increasing upwards, and local presence of carbonate nodules parallel to stratification. Its stratotype lies along the right bank of the Tagus River (GPS: N39º46'51.13'', W5º44'48.71''), close to the Almaraz nuclear power plant, named Arrocampo by García-Hidalgo (1985). The base of the formation contains the earliest ichnofossils assigned to *Treptichnus pedum* (Fig. 18B-C), so marking the chronostratigraphic base of the Terreneuvian, although the appearance coincides with the occurrence of siliciclastic sediments and so is clearly facies controlled.

ACKNOWLEDGEMENTS

References

Álvarez-Nava Oñate, H.; García Casquero, J.L.; Gil Toja, A.; Hernández Urroz, J.; Lorenzo Álvarez, S.; López Díaz, F.; Mira López, M.; Monteserín López, V.; Nozal Martín, F.; Pardo Alonso, M.V.; Picart Boira, J.; Robles Casas, R.; Santamaría Casanovas, J. & Solé, F.J. (1988). Unidades litoestratigráficas de los materiales Precámbrico-Cámbricos en la mitad suroriental de la zona Centro-Ibérica. II Congreso Geológico de España, Comunicaciones, 1: 19–22.

Álvaro, J.J.; Cortijo, I.; Jensen, S.; Lorenzo, S.; Palacios, T. & Pieren, A. (2019). Updated stratigraphic framework and biota of the Ediacaran and Terreneuvian in the Alcudia-Toledo Mountains of the Central Iberian Zone, Spain. Estudios Geológicos, 75 (2): e093.

Bingen, B.; Griffin, W.L.; Torsvik, T.H. & Saeed, A. (2005). Timing of Late Neoproterozoic glaciation on Baltica constrained by detrital zircon geochronology in the Hedmark Group, south-east Norway. Terra Nova, 17: 250–258 https://doi.org/10.1111/j.1365-3121.2005.00609.x

Bowring, S.A.; Landing, E.; Myrow, P. & Ramezani, J. (2002). Geochronological constraints on terminal Neoproterozoic events and the rise of metazoans. Astrobiology, 2: 457–458.

Brasier, M.D.; Perejón, A.; & de San José, M.A. (1979). Discovery of an important fossiliferous Precambrian-Cambrian sequence in Spain. Estudios Geológicos, 35: 379–383. https://doi.org/10.1016/0031-0182(79)90092-0

Condon, D.J. & Bowring, S.A. (2011). A user's guide to Neoproterozoic geochronology. Geological Society, London, Memoirs, 36:135–149. https://doi.org/10.1144/M36.9

Cortijo, I., Martí Mus, M., Jensen, S. & Palacios, T. (2010). A new species of *Cloudina* from the terminal Ediacaran of Spain. Precambrian Research, 176: 1–10.

Cortijo, I., Mus, M.M, Jensen, S. & Palacios, T. (2015). Late Ediacaran skeletal body fossil assemblage from the Navalpino anticline, central Spain. Precambrian Research, 267: 186–195.

Eyles, N. (1990) Marine debris flows: Late precambrian "tillites" of the Avalonian-Cadomian orogenic belt. Palaeogeography, Palaeoclimatology, Palaeoecology, 79: 73–98. https://doi.org/10.1016/0031-0182(90)90106-H

Gámez Vintaned, J.A. (1996). The río Huso section. In: Field Trip guide and Abstracts, II Field Conference of the Cambrian Stage Subdivision Working Groups (Liñán, E.; Gámez Vintaned, J.A. & Gozalo, R., Eds.), Zaragoza University Press, Zaragoza, 28–31.

Gámez Vintaned, J.A. & Liñán, E. (1996). Significant ichnological data during the Neoproterozoic-early Cambrian transition in Iberia. In: Field Trip guide and Abstracts, II Field Conference of the Cambrian Stage Subdivision Working Groups (Liñán, E.; Gámez Vintaned, J.A. & Gozalo, R., Eds.), Zaragoza University Press, Zaragoza, 101–102.

Gámez Vintaned, J.A. & Liñán, E. (2007). The Precambrian-Cambrian boundary in Spain: ichnofossil palaeobiology and zonation. In: The Rise and Fall of the Vendian (Ediacaran) Biota. Origin of the Modern Biosphere (Semikhatov, M.A., Ed.). Geos, Moscow, 54–57.

García Hidalgo, J.F. (1985). Estratigrafia y sedimentologia del Alcudiense Superior en los anticlinorios de Ibor y Navezuelas-Robledollano. Seminarios de Estratigrafía, 12: 1–190.

García-Hidalgo, J.F.; Pieren Pidal, A.P.; Olivé Davó, A.; Carbajal Menéndez, A.; de la Fuente Krauss, J.V.; Moreno, F.; Cantos Robles, R. & Liñán, E. (1993). Mapa Geológico de España a escala 1:50.000 (2ª Serie). Memoria de la Hoja 779 - Villanueva de La Serena. IGME, Madrid.

Graindor, M.J. (1964). Les tillites anté-cambriennes de Normandie. Geologische Rundschau, 54: 61–82. https://doi.org/10.1007/BF01821170

Halverson, G.P.; Hoffman, P.F.; Schrag, D.P.; Maloof, A.C. & Rice, A.H.N. (2005). Toward a Neoproterozoic composite carbon isotope record. Geological Society of America Bulletin, 117: 1181–1207. https://doi.org/10.1130/B25630.1

Jensen, S. & Palacios, T. (2016). The Ediacaran-Cambrian trace fossil record in the Central Iberian Zone, Iberian peninsula. Comunicaçoes Geológicas, 103: 83–92.

Jensen, S.; Palacios, T. & Martí Mus, M. (2007). A brief review of the fossil record of the Ediacaran-Cambrian transition in the area of Montes de Toledo-Guadalupe (Spain). In: The Rise and Fall of the Ediacaran Biota (Vickers-Rich, P. & Komarover, P. eds). Geological Society, London, Special Publications, 286: 223–235. https://doi.org/10.1144/SP286.16

Julivert, M.; Fontboté, J.M.; Ribeiro, A. & Conde, L.S. (1972). Mapa Tectónico de la Península Ibérica y Baleares a escala 1:1.000.000 y Memoria Explicativa. IGME. Madrid.

Karaoui, B.; Breitkreuz, C.; Mahmoudi, A.; Youbi, N.; Hofmann, M.; Gärtner, A. & Linnemann, U. (2015). U-Pb zircon ages from volcanic and sedimentary rocks of the Ediacaran Bas Draâ inlier (Anti-Atlas Morocco): Chronostratigraphic and provenance implications. Precambrian Research, 263: 43–58. https://doi.org/10.1016/j.precamres.2015.03.003

Letsch, D.; Large, S.J.E.; Buechi, M.W.; Winkler, W. & von Quadt, A. (2018). Ediacaran glaciations of the West African Craton - evidence from Morocco. Precambrian Research, doi: https://doi.org/10.1016/j.precamres.2018.02.015

Linnemann, U.; Pieren Pidal, A.; Hofmann, M.; Drost, K.; Quesada, C.; Gerdes, A.; Marko, L.; Gärtner, A.; Zieger, J.; Ulrich, J.; Krause, R. & Horak, J. (2018). A ~565 Ma old glaciation in the Ediacaran of peri-Gondwanan West Africa. International Journal of Earth Sciences, 107: 885–911. https://doi.org/10.1007/s00531-017-1520-7

Liñán, E.; Perejón, A. & Sdzuy, K. (1993). The Lower-Middle Cambrian stages and stratotypes from the Iberian Peninsula: A revision. Geological Magazine, 130: 817–833. https://doi.org/10.1017/S0016756800023189

Liñán, E.; Gozalo, R.; Palacios, T.; Gámez Vinaned, J.A.; Ugidos, J.M. & Mayoral, E. (2002). Cambrian. In: The Geology of Spain (Gibbons, W. & Moreno, T., Eds.). Geological Society, London, 17–29. https://doi.org/10.1144/GOSPP.3

Ovtracht, A. & Tamain, G. (1970). Essai tectonique en Sierra Morena (Espagne). Congrès national des sociétés savantes. Sciences, Reims, C 95 (1): 305–327.

Palacios Medrano, T. (1989). Microfósiles de pared orgánica del Proterozoico superior (región central de la Península Ibérica). Memorias del Museo Paleontológico de la Universidad de Zaragoza, 3: 1–91.

Pieren, A.P. (2000). Las sucesiones anteordovícicas de la región oriental de la provincia de Badajoz y área contigua de la de Ciudad Real. PhD, Universidad Complutense Madrid.

Pu, J.P.; Bowring, S.A.; Ramezani, J.; Myrow, P.; Raub, T.D.; Landing, E.; Mills, A.; Hodgin, E. & Macdonald, F.A. (2016). Dodging snowballs: Geochronology of the Gaskiers glaciation and the first appearance of the Ediacaran biota. Geology, 44: 955–958. https://doi.org/10.1130/G38284.1

San José, M.A. de, Pieren Pidal, A.P.,García-Hidalgo, J.F., Vilas Minondo, L., Herranz Araújo, P., Peláez Pruneda, J.R. & Perejón, A. (1990). Ante-Ordovician stratigraphy. In: Pre-Mesozoic Geology of Iberia (Dallmeyer, R.D. & Martínez García, E., Eds.), Springer, Berlin: 147–159.

Talavera, C.; Montero, P.; Martínez Poyatos, D. & Williams, I.S. (2012). Ediacaran to Lower Ordovician age for rocks ascribed to the Schist-Graywacke Complex (Iberian Massif, Spain): Evidence from detrital zircon SHRIMP U-Pb geochronology. Gondwana Research, 22: 928–942. https://doi.org/10.1016/j.gr.2012.03.008

Thompson, M.D.; Ramezani, J. & Crowley, J.L. (2014). U-Pb zircon geochronology of Roxbury Conglomerate, Boston Basin, Massachusetts: Tectono-stratigraphic implications for Avalonia in and beyond SE New England. American Journal of Science, 314(6): 1009–1040. https://doi.org/10.2475/06.2014.02

Vernhet, E.; Youbi, N.; Chellai, E.H.; Villeneuve, M. & El Archi, A. (2012). The Bou-Azzer glaciation: Evidence for an Ediacaran glaciation on the West African Craton (Anti-Atlas, Morocco). Precambrian Research, 196–197: 106–112. https://doi.org/10.1016/j.precamres.2011.11.009

Vickers-Rich, P.; Ivantsov. A.; Kattan, F.H.; Johnson, P.R.; Al Qubsani, A.; Kashghari, W.; Leonov, M.; Rich, T.; Linnemann, U.; Hofmann, M.; Trusler, P.; Smith, J.; Yazidi, A.; Rich, B.; Al Garni, S.M.; Shamari, A.; Al Barakati, A. & Al Kaff, M.H. (2012). In search of the Kingdom's Ediacarans: The first genuine Metazoans (macroscopic body and trace fossils) from the Neoproterozoic Jibalah Group (Vendian/Ediacaran) on the Arabian Shield. Saudi Geological Survey Technical Report, SGS-TR-2013-5: 1–21.

Vidal, G.; Palacios, T.; Gámez-Vintaned, J.A.; Díaz Balda, M.A. & Grant, S.W.F. (1994). Neoproterozoic-early Cambrian geology and palaeontology of Iberia. Geological Magazine, 131: 729–765. https://doi.org/10.1017/S001675680001284X

Wegmann, C.E.; Dangeard, L. & Grauindor, M.J. (1950). Sur quelques caractères remarquables de la formation précambrienne connue sous le nom de poudingue de Granville. Comptes Rendus de l'Académie des Sciences, Paris, 230: 979–980.

Wegmann, C.E. (1951). Subkambrische Tillite in der herzynischen Faltungszone. Geologische Rundschau, 39: 221–234. https://doi.org/10.1007/BF01803322